Estimating intensity variance due to noise in registered images

Gustavo K. Rohde,[1,2] Alan S. Barnett[3], Peter J. Basser[1], Carlo Pierpaoli[1]

[1]STBB/LIMB/NICHD, National Institutes of Health, Bethesda, MD, USA.

[2]Applied Mathematics and Scientific Computation Program, University of Maryland, MD, USA.

[3]NIMH, National Institutes of Health, Bethesda, MD, USA

ABSTRACT

Image registration refers to the process of finding the spatial correspondence between two or more images. This is usually done by applying a spatial transformation, computed automatic or manually, to a given image using a continuous image model computed either with interpolation or approximation methods. We show that noise induced signal variance in interpolated images differs significantly from the signal variance of the original images in native space. We describe a simple approach to compute the signal variance in registered images based on the signal variance and covariance of the original images, the spatial transformations computed by the registration procedure, and the interpolation or approximation kernel chosen. Our approach is applied to diffusion tensor (DT) MRI data. We show that incorrect noise variance estimates in registered diffusion weighted images can affect the estimated DT parameters, their estimated uncertainty, as well as indices of goodness of fit such as chi-square maps. In addition to DT-MRI, we believe that this methodology would be useful any time parameter extraction methods are applied to registered or interpolated data.

Keywords: Image registration, interpolation, variance, noise, parameter estimation.

1. INTRODUCTION

Post-acquisition image alignment (registration) is routinely performed in biomedical research and clinical practice[1,2]. Applications using image registration techniques include motion and distortion correction in functional MRI (fMRI), diffusion tensor MRI (DT-MRI), and MR relaxometry experiments. In addition, image registration procedures are increasingly being used in computational based studies of neuroanatomy. This involves understanding the variability of tissue properties, including shape, across specific populations. An example is voxel-based morphometry, described in[3].

In general, many of the current post-processing methodologies can be summarized as follows. A set of medical images is acquired and reconstructed using standard methodologies. This step may include: filtering to avoid "ringing" artifacts, denoising, intensity corrections, etc. Next, using one of many available algorithms, images are registered to ensure, as much as possible, that a fixed image coordinate corresponds to the same structure, or anatomical coordinate, in all images acquired. This step is necessary because the subject being imaged may move during data acquisition. In addition, images may contain geometric distortions with respect to each other. In echo planar (EPI) MRI these distortions can be caused by magnetic field susceptibility related artifacts. In EPI-based diffusion weighted imaging, significant geometric distortions may also occur due to eddy-currents induced by the rapidly switched diffusion weighting magnetic field gradients applied during imaging. Corrections to account for such misregistration artifacts are absolutely necessary to ensure the data analysis is reliable. In addition to correcting for motion and geometric distortions, the entire image sequence may also be aligned to a standard template image, using stereotaxic normalization techniques, for example, so that the data analysis results can be more conveniently interpreted. Data analysis consists of extracting or estimating some physically meaningful parameters from the sequence of medical images. In DT-MRI a 3x3 symmetric diffusion tensor is estimated, based on which several other quantities such as measures of diffusion anisotropy and depictions of fiber tracts can be generated. In fMRI, these may be statistical parametric maps[4], for example.

In many of these applications the analysis of the registered images involves fitting or estimating model parameters from the intensity values of the images. For such tasks it is crucial to know the correct signal variance of the *registered* images so that least-squares procedures, for example, can be properly implemented. Though significant research has been devoted to estimating signal variance in medical images--some examples in MRI include[5-7] among others--it is important to recognize that the signal variances in the registered and the original unregistered images differ. This is because the image interpolation or approximation step generally required in image registration can, as will be shown later, significantly change the noise properties of the image. We will show how a simple formula can be used to compute the appropriate signal variance in registered images. The analysis of diffusion weighted MRI data using the diffusion tensor model will be used as a case study. That is, given a set of diffusion weighted MR images (DWI) we use an existing software to register the DWIs to remove rigid body motion and eddy-current related distortions prior to tensor computation. We then show that noise variance in the registered images differs from the noise variance in the original images. However, even though DT-MRI is the only application discussed in detail in this paper, we believe that the general approach described in this paper should be considered whenever registered images are being analyzed using procedures that require knowledge of the variance in the image intensity values.

At the time of writing not much related work can be found in the biomedical imaging literature. Friston *et al*[8] address the problem of removing movement- related artifacts, such as those caused by intensity fluctuations due to the change in position of the imaged object with respect to the reference frame of the scanner. In other works[9,10] the authors investigate the error in the intensity values produced by interpolation procedures applied on the registered images. Maas and Renshaw[11] discuss artifacts related to high frequency losses on registered (interpolated) data. Pluim *et al.* report that interpolation methods may cause undesirable artifacts when estimating the Mutual Information similarity measure[12]. Nickerson *et al.*[13] describe a method through which the local intensity variance in positron emission tomography (PET) can be estimated from the operations performed during image reconstruction. None of these works, however, detail the importance of, and methods for obtaining correct estimates of the signal variance at each coordinate of each registered image.

In the field of diffusion weighted imaging and diffusion tensor MRI, several researchers have investigated methods for performing post-acquisition motion and distortion correction of DWI data[14-19]. Though the registration methods differ, most of these works use linear interpolation to produce the series of DWIs. This series is then used to estimate one diffusion tensor for each voxel via least- squares fitting procedures similar to the χ^2 minimization procedure described in[20]. We show in this paper that least-squares fitting procedures that extract diffusion tensor estimates from registered data can be affected by the changes in image noise properties due to interpolation. We also provide a simple method for obtaining correct variance estimates for the registered images.

2. THEORY

In practice, the process of registering two images is usually approached within an optimization framework in which the goal is to find a spatial transformation $f(\mathbf{x})$, where $f : \Re^2 \to \Re^2$, or $f : \Re^3 \to \Re^3$ for volumetric images, that maximizes some similarity measure I between the digitized target $T(\mathbf{x})$ and source $S(\mathbf{x})$ images:

$$\max_f I\big(S(f(\mathbf{x})), T(\mathbf{x})\big). \tag{1}$$

The function $f(\mathbf{x})$ may be a rigid body, affine, or higher order transformation, depending on the application. The function I usually measures the similarity between the images being registered by computing some form of statistical dependency between the intensity values of the images. In the processing pipeline described above, the problem defined by equation
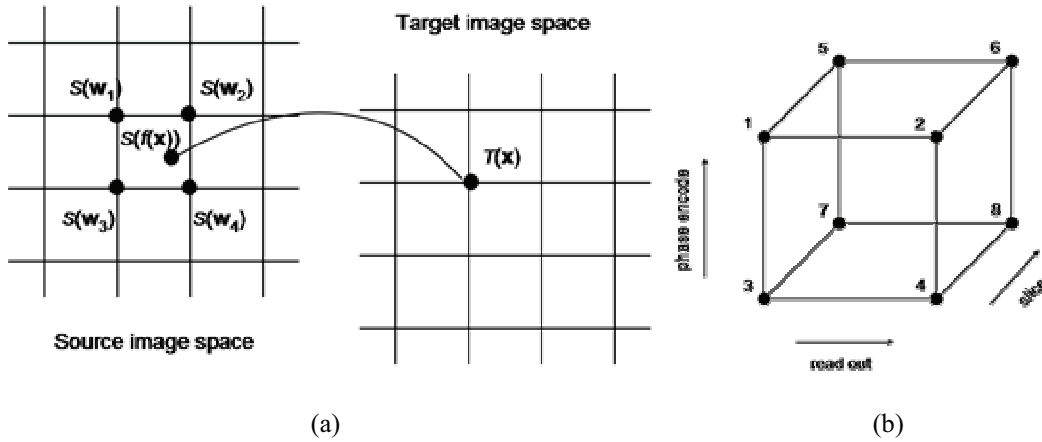
Figure 1: Part (a), schematic diagram depicting the process of interpolation performed for image registration. A coordinate in the target image space is transferred to a coordinate in the source image space. The value of the image at the source image space coordinate is computed based on the intensity values of the sampling coordinates around it. Part (b): diagram depicting the order of points used in the definition of the covariance matrix of the data.

(1) is usually solved for K images in the image sequence $\{S_1(\mathbf{x}), \ldots, S_K(\mathbf{x})\}$, so it is clear that the sequence of images $\{S_1(f_1(\mathbf{x})), S_k(f_k(\mathbf{x})), \ldots, S_K(f_K(\mathbf{x}))\}$ is properly aligned. Note that in cases where $f_k(\mathbf{x})$ is used to correct for geometric distortions caused by imperfect magnetic field gradients in MRI, for example, the intensity value of the corrected images may also have to be multiplied by a correction factor[19,21]:

$$\tilde{S}_k\left(f_k(\mathbf{x})\right) = S_k\left(f_k(\mathbf{x})\right)\det\left|Jac\left(f_k(\mathbf{x})\right)\right|, \tag{2}$$

where $\det\left|Jac\left(f_k(\mathbf{x})\right)\right|$ stands for the determinant of the Jacobian matrix of the transformation $f_k(\mathbf{x})$.

Independently of how the solution to equation (1) is actually computed for each image in the sequence, many imaging applications require knowing the value of the registered images $\{S_1(f_1(\mathbf{x}_i)), \ldots, S_K(f_K(\mathbf{x}_i))\}$ for some arbitrary coordinate $\mathbf{x}_i$. Since in general the point $f_k(\mathbf{x})$ will not coincide with a sampling coordinate of image S_k, an interpolation or approximation strategy must be used to produce the image value $S_k(f_k(\mathbf{x}))$. Many approximation and interpolation methods can be chosen to perform such tasks[22]. Most estimate the value of $S_k(f_k(\mathbf{x}))$ based on a linear combination of the intensity values of image S_k around the point $f_k(\mathbf{x})$. Figure 1(a) illustrates this process. Note that $\mathbf{w}$ refers to grid coordinates of the image S_k. Mathematically, this interpolation or approximation procedure can be expressed as:

$$S_K\left(f_K(\mathbf{x})\right) = \sum_{\mathbf{w}_i \in \Theta} \alpha_i S_K\left(\mathbf{w}_i\right), \tag{3}$$

where Θ defines a set of sampling coordinates that surround $f(\mathbf{x})$ (see Figure 1(a)). The coefficients α_i of the linear combination (3), as well as the size of Θ are determined solely by the choice of interpolation or approximation kernel. For the linear interpolation method, one of the most popular image interpolation methods, the value of the image S at coordinate $f(\mathbf{x})$ is given by:

,

$$S(f(\mathbf{x})) = \sum_{i=1}^{2}\sum_{j=1}^{2}\sum_{k=1}^{2}(1-V_i)(1-P_j)(1-Q_k)S(x_i, y_j, z_k) \tag{4}$$

where $V_i = |f(\mathbf{x})_x - x_i|$, $P_j = |f(\mathbf{x})_y - y_j|$, $Q_k = |f(\mathbf{x})_z - z_k|$, and $\{x_i, y_j, z_k\}$ are image grid coordinates for which $|f(\mathbf{x})_x - x_i| < 1$, $|f(\mathbf{x})_y - y_i| < 1$, $|f(\mathbf{x})_z - z_i| < 1$. Thus the coefficients of the linear combination (3) are given by:

$$\alpha_{i,j,k} = (1-V_i)(1-P_j)(1-Q_k). \tag{5}$$

The set Θ, in this case, are the coordinates $\mathbf{w}_i$ for which $|f(\mathbf{x}) - \mathbf{w}_i| \le 1$ holds. Naturally, when different interpolation or approximation methods are used, different formulas are needed for estimating the variance of any given interpolated image value. In general, the coefficients of the linear combination (3) can be written in terms of sampled values of the interpolation kernel being used.

Because of random variability introduced at several steps during image acquisition, the measurement $S_k(\mathbf{w}_i)$ should be considered a random variable with a variance $\mathrm{Var}(S_k(\mathbf{w}_i))$. For MR images it is customary to assume that noise variance, denoted by λ^2, is uniform throughout the imaging volume. Note that, though it can be assumed that $S_k(\mathbf{w}_i)$ and $S_k(\mathbf{w}_j)$, where $i \ne j$, have equal variances, in general they are not independent measurements because several image reconstruction steps effectively correlate measurements from different image coordinates. Correlation in the data due to the reconstruction procedure can arise from filtering during analog to digital conversion, filtering to remove ringing artifacts, filtering to remove noise, correcting for ghosting artifacts (particularly salient in EPI reconstructions), and others. Correlation between values in different image coordinates occurs not only in MRI, but X-ray based computed tomography and positron emission tomography (PET) also. This is because most reconstruction algorithms use filtering operations that correlate intensity values of different image coordinates. A simple method for estimating this correlation in MRI will be described in the next section.

In short, because of the noise variability introduced during image acquisition and processing, the measurements $S_k(\mathbf{w}_i)$ and $S_k(\mathbf{w}_j)$ are random variables with variance $\mathrm{Var}(S_k(\mathbf{w}_i))$ and $\mathrm{Var}(S_k(\mathbf{w}_j))$, respectively, and covariance $\mathrm{Cov}(S_k(\mathbf{w}_i), S_k(\mathbf{w}_j))$. Thus, $S_k(f_k(\mathbf{x}))$, as defined by equation (3), is also a random variable with variance[23]:

$$\mathrm{Var}(S_k(f_k(\mathbf{x}))) = \left(\sum_{\mathbf{w}_i \in \Theta}\alpha_i^2 \mathrm{Var}(S_k(\mathbf{w}_i))\right) + 2\left(\sum_{\{\mathbf{w}_i,\mathbf{w}_j\}\in\Theta, i<j}\alpha_i\alpha_j\mathrm{Cov}(S_k(\mathbf{w}_i), S_k(\mathbf{w}_j))\right). \tag{6}$$

If it can be assumed that $\mathrm{Var}(S_k(\mathbf{w}_i)) = \lambda^2$ is approximately constant for all values of the image (this is often the case in the foreground of MR images at high signal to noise ratios) (6) simplifies to,

$$\mathrm{Var}(S_k(f_k(\mathbf{x}))) = \lambda^2\left(\sum_{\mathbf{w}_i \in \Theta}\alpha_i^2\right) + 2\left(\sum_{\{\mathbf{w}_i,\mathbf{w}_j\}\in\Theta, i<j}\alpha_i\alpha_j\mathrm{Cov}(S_k(\mathbf{w}_i), S_k(\mathbf{w}_j))\right). \tag{7}$$

In cases when the intensity correction function defined in (2) needs to be applied to the registered image $S_k(f_k(\mathbf{x}))$ to obtain intensity corrected value $\tilde{S}_k(f_k(\mathbf{x}))$, it is easy to show that the correct formula for the variance becomes:

$$\text{Var}\left(\tilde{S}_k(f_k(\mathbf{x}))\right) = \left(\det|Jac(f_k(\mathbf{x}))|\right)^2\left(\lambda^2\left(\sum_{i\in\Theta}\alpha_i^2\right) + 2\left(\sum_{\{i,j\}\in\Theta,i<j}\alpha_i\alpha_j\text{Cov}\left(S_k(\mathbf{w}_i),S_k(\mathbf{w}_j)\right)\right)\right). \qquad (8)$$

Next we show that formula (8) is necessary when quantitative analysis, such as estimation of an effective diffusion tensor, is to be performed on registered data.

3. METHODS

3.1. Diffusion weighted MRI data acquisition

The data sets in the demonstrations used throughout this paper were acquired with a standard single-shot multi-slice spin-echo EPI sequence (i.e.: fat suppression pulse, 90 degree pulse, first diffusion gradient, 180 degree pulse, second diffusion gradient, EPI readout). Scans were performed on a 1.5 T GE Signa system equipped with a whole-body gradient coil able to produce gradient pulses up to 50 mT/m (GE Medical Systems, Milwaukee, WI). The imaged volume was composed of 80 contiguous slices with 2 mm slice thickness and 2 mm in-plane resolution. The echo-time was 82.7 ms, the read-out time 50 ms, and the repetition time was greater than 10 s with cardiac gating (4 acquisitions per heart beat starting with a 150 ms delay after the rise of the sphygmic wave as measured with a peripheral pulse oxymeter). The gradient strength was 49 mT/m, yielding a b value (i.e., trace of the b-matrix) of 1,120 s/mm^{2}. A total of 56 3D images were acquired by repeating 8 times a diffusion sampling scheme described previously[24] which includes one volume with no diffusion weighting followed by the same volume six times, acquired with diffusion gradients applied in different directions. The total imaging time was approximately 20 minutes. Replicate volumes were acquired for signal to noise considerations in order to improve the quality of the estimated diffusion tensor parameters. The signal to noise ratio, as measured by the mean signal in the region of the thalamus divided by the estimated standard deviation of the signal (see section below), was about 13 for the T2-weighted images and about 7 for the diffusion weighted images.

3.2. MRI noise estimation

The sources that introduce uncertainty in each voxel intensity are many and are generally put into one of two categories: thermal noise, and physiological noise. Other sources may also exist in the electronics of the acquisition system, such as digitization etc., but these can be minimized in an ideal experiment. Thermal noise is usually considered as "white noise" because it is expected that its power should be equal for all frequencies within the readout bandwidth. Because the images are reconstructed using the Fourier transform, the variance that characterizes the uncertainty due to thermal noise is constant throughout the imaging volume[25]. Typically, however, the image analysis process is done on the magnitude of the data that has been reconstructed with the Fourier transform. This causes the noise induced variance in the background regions of magnitude reconstructed images to be lower than the variance in the foreground of the images. We estimate the variance of the signal in foreground of the images by computing the variance of magnitude reconstructed intensity values in an artifact-free background region and propagating it to regions with strong signal from the brain through the method described in[5,6].

The correlation matrix used in our experiments was estimated empirically. Though theoretically possible, it could be very cumbersome to account for all of the filtering steps applied to the data before it becomes a magnitude image. In addition, some steps taken during analog to digital conversion of the free induction decay signals may be proprietary and thus inaccessible. Instead, we acquired and reconstructed several 3D images of pure noise. Using this pure noise image data we

computed the correlation coefficient between the original volumes and the same volumes shifted by one pixel in the x, y, and z directions. Note that because we are using linear interpolation, it is only necessary to include 1 voxel shift in the computation (8). When bases functions of wider support are used in the interpolation or approximation procedure, the correlations of larger shifts may be required. Using this method, we computed the following 8x8 correlation matrix:

$$
Corr(i, j) = \begin{bmatrix}
1 & 0.35 & 0.40 & 0.25 & 0 & 0 & 0 & 0 \\
0.35 & 1 & 0.25 & 0.40 & 0 & 0 & 0 & 0 \\
0.40 & 0.25 & 1 & 0.35 & 0 & 0 & 0 & 0 \\
0.25 & 0.40 & 0.35 & 1 & 0 & 0 & 0 & 0 \\
0 & 0 & 0 & 0 & 1 & 0.35 & 0.40 & 0.25 \\
0 & 0 & 0 & 0 & 0.35 & 1 & 0.25 & 0.40 \\
0 & 0 & 0 & 0 & 0.40 & 0.25 & 1 & 0.35 \\
0 & 0 & 0 & 0 & 0.25 & 0.40 & 0.35 & 1
\end{bmatrix}.
\tag{9}
$$

Figure 1(b)--which defines the ordering of the voxel coordinates--helps explain the correlation matrix expressed in (9). Because we are assuming that most of the correlation is caused by linear filtering operations applied on the image data, the noise correlation matrix (9) should be approximately constant throughout the domain of the original magnitude reconstructed images. Note that since our acquisition is based on a 2D EPI pulse sequence, measurements between one slice and the next show no significant correlation. Also note that the correlations in the x, and y directions are not equal, since additional operations are performed in the phase encode (y in this case) direction to minimize ghosting artifacts. Lastly, since we are also assuming that the noise variance in the original magnitude reconstructed image is constant, the covariance matrix used in (8) is given by:

$$
Cov(i, j) = Corr(i, j) \times \lambda^2 .
\tag{10}
$$

3.3. Diffusion tensor estimation

The diffusion tensor model was estimated in each voxel $\mathbf{x}$ from the diffusion weighted data by minimizing the following equation:

$$
\chi^2\left(\mathbf{D}(\mathbf{x}), A(\mathbf{x})\right) = \frac{1}{K-7} \sum_{k=1}^{K} \frac{\left(A(\mathbf{x})e^{(-\mathbf{D}(\mathbf{x}):\mathbf{b}_k)} - \tilde{S}_k\left(f_k(\mathbf{x})\right)\right)^2}{\mathrm{Var}\left(\tilde{S}_k\left(f_k(\mathbf{x})\right)\right)},
\tag{11}
$$

where $\mathbf{D}(\mathbf{x})$ is a 3x3 symmetric matrix, $A(\mathbf{x})$ is the amplitude term, and $\mathbf{b}_k$ is the b-matrix for image k, and $\mathbf{D}:\mathbf{b}$ stands for the matrix dot product[20]. The minimization was performed using the Levenberg-Marquardt least-squares method.

3.4. Simulation experiments

As an initial test of our variance estimation software we performed simulation experiments using artificially constructed data. In this experiment, one hundred 2D images of Gaussian distributed random noise with mean zero and variance one were rotated about their centers by 5 degrees using bilinear interpolation. In this simulation, the correlation between the noisy values of any two coordinates was approximately zero. For a fixed pixel coordinate $\mathbf{x}$ the variance across all of the

(a)   (b)   (c)   (d)
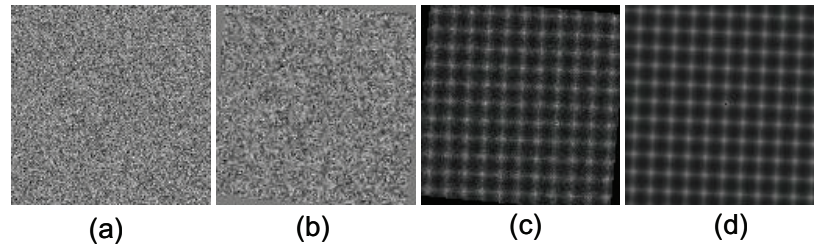
Figure 2: Simulation showing how the interpolation necessary to relate measurements in two images can significantly affect the noise properties of the interpolated image. Part (a): an image of simulated noise. Part (b) is the image in part (a) rotated by 5 degrees. Part (c) is the variance of image (b) computed by repeating the rotation experiment 100 times. Part (d) shows the variance of image (b) predicted by formula (8).

rotated images was computed and displayed. The purpose of this experiment is to show that the variance in the images acquires a particular striped structure. We show that by using equation (8), the variance in the interpolated images can be predicted exactly.

3.5. Real data experiments

The diffusion weighted data used in the examples in this paper were registered to account for patient motion and eddy-current induced geometric distortions using the methodology described in[19]. The details about the registration algorithm being used are not particularly relevant. Only that, once the spatial transformations that register the set of DW images are calculated, the output images are computed using trilinear interpolation.

The diffusion tensor at each voxel was computed using the registered images by solving equation (11) as described above. For comparison purposes, we also estimate the diffusion tensor from the registered images using equation (11), but using a constant term for the noise variance $\mathrm{Var}\left[\tilde{S}_k\left(f_k(\mathbf{x})\right)\right] = \lambda^2$. We then compare several relevant quantities derived from the estimated diffusion tensor computed with and without formula (8), including the trace, fractional anisotropy, and χ^2 errors.

4. RESULTS

The results of the simulation experiments are shown in Figure 3. Part (a) shows a sample noisy image computed as described above. Part (b) shows the same image rotated by 5 degrees about its center. Part (c) shows an image of the variance of the one thousand rotated images computed at each pixel. Clearly the variance became non-uniform and acquired a striped pattern throughout the domain of the image. This variance image was computed analytically using formula (7), and the result is shown in part (d).

A similar effect can be seen in real data experiments using diffusion weighted images. Though these striped artifacts are practically invisible in the individual interpolated DWI volumes, they become evident in the χ^2 maps computed using equation (11). Some results are shown in Figure 3. In this experiment a set of DWI volumes was rotated about its horizontal axis by about 7.5 degrees, thus causing interpolation to be performed between values of different slices, as well as between values of different lines in the logical *y* direction. For this experiment, the same rotation transformation was

(a)   (b)   (c)
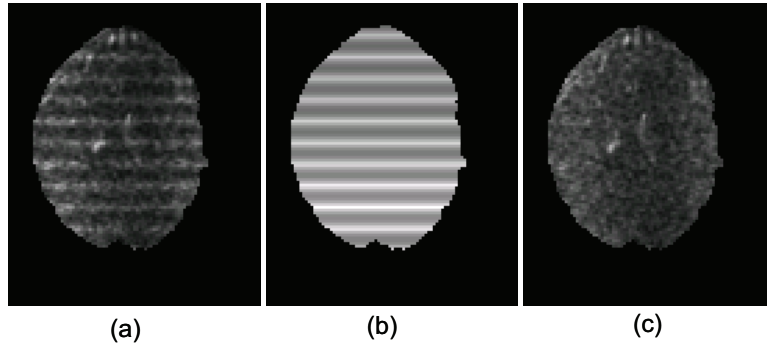
Figure 3: Demonstration of bias in χ^2 between the DT model and registered DWI data. Part (a) show the χ^2 map computed using a single value for the variance in the data. Part (b) shows the non-uniform variance estimated using formula (8). Part (c) shows the same χ^2 map, however, this time computed using the variance values displayed in part (b).

applied to each DWI volume, that is: $f_1(\mathbf{x})=f_k(\mathbf{x}) \ldots =f_K(\mathbf{x})$. Part (a) of Figure 3 shows the χ^2 map computed using a single value, λ^2, for the variance of each voxel in each image. Horizontal stripes are visible along the vertical axis of the image, reflecting the different amounts of interpolation performed at each voxel location. Part (b) shows the variance predicted using eq. (8). Part (c) shows the χ^2 map computed using the variance given by eq. (8). The "striping" patterns become negligible when compared to those shown in part (a) of the same figure. Note that the dynamic ranges of both χ^2 maps in this example were auto-scaled to obtain maximum contrast.

We also compared some of the most well known parameters derived from the diffusion tensor computed from the fitting of eq. (11). For reference, the amplitude image, *A* in formula (11), is shown in figure 4. Figure 5(a) shows the relative error between the trace parameter computed with and without the variance correction scheme proposed above. The relative error was computed using the following formula: $|v_{corrected}-v_{uncorrected}|/ v_{corrected}$, where '*v*' stands for the voxel's specific value for the trace of the diffusion tensor. The absolute value of the difference between the fractional anisotropy values computed with and without the variance correction described above is shown in part (b) of figure 5.

5. DISCUSSION

The rotation experiments performed with the simulated noisy images demonstrate qualitatively and quantitatively the effect that image interpolation can have on the noise variance in registered or interpolated images. The experiment also shows that formula (8) can be used to estimate the variance in the interpolated images if the initial covariance matrix of the sampled image is known.

Experiments using real DWIs showed that the change of image noise properties caused by the registration (interpolation) procedure can significantly affect parameter estimation procedure in DT-MRI. First, the alignment of the entire DWI dataset to a standard template can cause χ^2 maps to acquire a striped pattern if a single value for the image intensity variance is used during tensor estimation. The pattern can be explained by the non-uniform intensity variance introduced by the image interpolation step. The patterns disappear when the correct noise variance in each voxel of each image, given
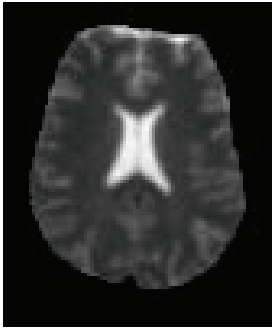
Figure 4: Amplitude image depicting the region in the brain where results are analyzed.

by equation (8), is used to compute the diffusion tensor. In our experience, the striped pattern in the χ^2 values is negligible if the DWI dataset is not aligned to a standard template, in addition to being corrected for motion and distortion, even if a single value for the intensity variance is used in estimating the tensor model. Nonetheless, formula (8) should be used in this case--because the images have suffered interpolation--to ensure an estimation of the correct variance values. In general the χ^2 computed from registered images is lower than the χ^2 computed from unregistered images when significant misregistration due to motion is present. However, the χ^2 values computed using a single variance value estimated from the original (unregistered) images were lower than the χ^2 values computed using equation (8) to estimate the correct intensity variance. This is to be expected since the variance of registered images at any given voxel location is less than or equal to the variance of the original (unregistered) images because of the interpolations 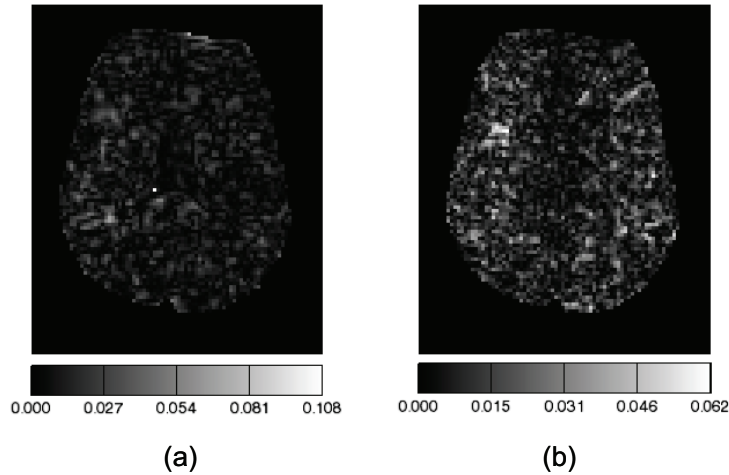necessary for registration. Thus, if a single variance value estimated from original (unregistered) images is used for the tensor computation, the overall effect will be an artificial decrease in the χ^2 maps derived from the tensor fitting.

We have also shown that the estimation of the trace and fractional anisotropy parameters of the diffusion tensor can be affected by incorrect noise variance estimates. In the experiment shown, the error between the parameters estimated with and without the variance correction to account for image registration was small: a few relative percentage points for the trace of the diffusion tensor and a few absolute percentage points for the fractional anisotropy index. We expect that the error caused by inappropriate weights in computing the actual parameters of the diffusion tensor model will be largest when the data being fit differs substantially from the model being used. To understand this, one only has to think of the extreme case in which the model fits the data without error. In this case, the weights being used become irrelevant since the numerator of the chi-squared equation becomes zero. The error between the data and the model arises from normally distributed thermal noise, physiological noise, as well as regions where it is known that the DT model poorly describes the underlying diffusion process, e.g. regions of crossing fibers. When considering only thermal, normally distributed additive noise, as we do throughout this paper, errors caused by incorrect variance estimates are not expected to be large and may diminish as the number of diffusion weighted images increases. As shown in the results section, however, these errors are expected to be in the order of a few percent.

The precise effect that changed image noise properties due to interpolation or approximation will have on DT estimation procedures cannot be determined *a priori* and will depend on several aspects of the registration and data processing procedures. Some of these are: the spatial transformations used to register the images, the interpolation or approximation kernel used, the noise variance and covariance in the original images, and the anatomical content of the images. However, it is worth noting that a translation of 0.5 pixels in all three dimensions can cause the variance of the signal to be reduced to 0.125 of the original variance of the signal when the linear interpolation method is used and if the data are spatially uncorrelated. If the correct noise variance value is not used, the resultant χ^2 measure will be underestimated by 8 times. Using the correlation matrix stated in equation (9) a translation of 0.5 pixels in all three dimensions would cause the variance in the interpolated image to be 0.25 of the variance in the original data. This would cause the χ^2 measure to be underestimated by 4 times if all images in the dataset suffered similar interpolation.

5.1. Implications for the analysis of variance of DT parameters

Figure 5: Part (a): relative error (absolute value of the difference divided by the 'correct' value) between the trace of the diffusion tensor computed with and without the variance estimate given by formula (8). Part (b): absolute value of the difference between fractional anisotropy values computed with and without the variance estimated by formula (8).

Knowledge of the uncertainty in the estimated diffusion tensor model parameters is important for assessing the significance of results of inter-subject or inter-acquisition comparisons. It is worth also noting that thermal noise variance not only plays a role in estimating the parameters of the model but also their uncertainty. From Basser *et al.*[20] it is known that when multivariate log-linear regression is used to compute the diffusion tensor parameters, the error variances of the estimated diffusion parameters are given by the diagonal elements of the matrix $\left(\mathbf{B^T}\Sigma_{\mathbf{e}}^{-1}\mathbf{B}\right)^{-1}$ where $\mathbf{B}$ is the "design" matrix for the experiment, computed from the vectors that define the diffusion weighting gradients being used, and the diagonal values of $\Sigma_{\mathbf{e}}^{-1}$ given by $\tilde{S}_k{}^2/Var(\tilde{S}_k)$, where $\tilde{S}_k$ represents the intensity value of the kth image (for a fixed spatial coordinate) in the experiment. As shown in appendix B, if incorrect values of $Var(\tilde{S}_i)$ are used the variance of the estimated parameters is no longer $\left(\mathbf{B^T}\Sigma_{\mathbf{e}}^{-1}\mathbf{B}\right)^{-1}$ and it is given by equation a modified version of it. Methods for estimating the uncertainty in parameters computed through nonlinear models usually rely on Monte Carlo-type simulations for which it is necessary to know the variance that characterizes the uncertainty of each image intensity value[26].

5.2. Implications for functional MRI and voxel based morphometry

Note that though we used diffusion tensor imaging as a case study, we believe that the same methodology could be used whenever data analysis requiring noise variance estimates is performed on registered or interpolated data. Some application examples in biomedical imaging include fMRI data analysis, studies of tissue shape and composition using statistical analysis of image data, MR relaxometry experiments, etc. In all such applications the goal is to detect image intensity changes that are the result of some biologically relevant phenomena. In fMRI this may be BOLD activation correlated with some type of brain activity, while in voxel based morphometry, for example, this may be information related to diseased tissue. Both fMRI data analysis and voxel based morphometry methods often rely on a generalized linear model for identifying the presence, absence, and quantification, of biologically relevant phenomena. In this framework the measured image data (at a fixed voxel coordinate), defined by an N dimensional vector $\mathbf{y}$, is modeled as a

linear combination of explanatory coefficients arranged in an NxM matrix $\mathbf{M}$ and unknown parameters defined by an M dimensional vector $\mathbf{a}$: $\mathbf{y}=\mathbf{Ma}+\mathbf{e}$, where $\mathbf{e}$ represents an N dimensional error vector whose entries are usually assumed to be independent, equally and normally distributed. If the error values are indeed normally distributed the maximum likelihood estimate for the model parameters is given by $\mathbf{a}=(\mathbf{M}^T\mathbf{M})^{-1}\mathbf{M}^T\mathbf{y}$, while the covariance matrix of the estimates is given by $\mathbf{S}_a = \mathbf{L}\,\mathbf{S}_y\mathbf{L}^T$, with $\mathbf{L}=(\mathbf{M}^T\mathbf{M})^{-1}\mathbf{M}^T$ and $\mathbf{S}_a$, $\mathbf{S}_y$ representing the covariance matrix of the estimated parameters and original data, respectively. Since the measurements $\mathbf{y}$ are usually assumed to be independently and identically distributed, the covariance matrix of the estimated parameters reduces to $\mathbf{S}_a = \lambda^2\,(\mathbf{M}^T\mathbf{M})^{-1}$, with λ^2 being the assumed noise variance. Note that this analysis is usually performed on registered images in order to account for patient motion and geometric distortions. As shown in this paper, since different images will have different spatial transformations (and thus different interpolation) applied on them, the constant noise variance assumption is no longer appropriate. That is, the variance due to noise of an image value that has suffered interpolation is expected to be different from the variance of an image value that has suffered no interpolation at all. At this point it is unclear what effect this will have on image analysis results obtained using the general linear model, though it is an issue that should be investigated further.

6. SUMMARY AND CONCLUSIONS

As fitting and estimation procedures from registered image data become increasingly more elaborate and quantitative, knowledge of the intensity variance due to noise will become more important for increasing the accuracy and scientific value of the results obtained from them. A method for estimating the variance in registered images is presented. The general approach can be summarized as follows. The output of the registration procedure is computed using an image interpolation or approximation procedure. The interpolation or approximation procedure can be written as a linear combination of the values of the image being registered. The coefficients of the linear combination are determined by the choice of interpolation or approximation kernel. Since the values of the image being registered are typically corrupted by noise, this operation can be viewed as a linear combination of random variables. The variance of the linear combination is given by well known statistical formulas.

The image interpolation or approximation generally required by image registration procedures will inevitably affect the noise variance properties of the images. We have shown that incorrect variance estimates can have a significant effect on diffusion tensor estimation procedures. The method we proposed for estimating the noise variance in registered images was shown to be successful in both simulated and real data experiments. Since χ^2 measures and noise variance estimates are used more and more frequently in diffusion data analysis--examples include image registration[14], diffusion model selection[27,28], robust tensor estimation[29], and brain tumor pathology detection[30]--correct variance estimates from registered image data will become increasingly important.

The methods described here could also be useful in other biomedical imaging applications such as MR relaxometry, fMRI data analysis, voxel based morphometry, etc. However, the effects of the technique in each of these applications are not discussed in detail here and could be the subject of future study. The techniques described here could also find applications in other image processing and data analysis fields such as automatic target recognition and segmentation of registered data obtained from satellite or other remote sensing machinery.

REFERENCES

1.   Pluim, J.P., J.B. Maintz, and M.A. Viergever, *Mutual-information-based registration of medical images: a survey.* IEEE Trans Med Imaging, 2003. **22**(8): p. 986-1004.
2.   Maintz, J.B. and M.A. Viergever, *A survey of medical image registration.* Med Image Anal, 1998. **2**(1): p. 1-36.
3.   Ashburner, J. and K.J. Friston, *Voxel-based morphometry--the methods.* Neuroimage, 2000. **11**(6 Pt 1): p. 805-21.
4.   Friston, K.J., et al., *Statistical Parametric Maps in Functional Imaging: A General Linear Approach.* Human Brain Mapping, 1995. **2**: p. 189-210.

5. Henkelman, R.M., *Measurement of signal intensities in the presence of noise in MR images.* Med Phys, 1985. **12**(2): p. 232-3.
6. Gudbjartsson, H. and S. Patz, *The Rician distribution of noisy MRI data.* Magn Reson Med, 1995. **34**(6): p. 910-4.
7. Sijbers, J., et al., *Estimation of the noise in magnitude MR images.* Magn Reson Imaging, 1998. **16**(1): p. 87-90.
8. Friston, K.J., et al., *Movement-related effects in fMRI time-series.* Magn Reson Med, 1996. **35**(3): p. 346-55.
9. Thacker, N.A., et al., *Improved quality of re-sliced MR images using re-normalized sinc interpolation.* J Magn Reson Imaging, 1999. **10**(4): p. 582-8.
10. Grootoonk, S., et al., *Characterization and correction of interpolation effects in the realignment of fMRI time series.* Neuroimage, 2000. **11**(1): p. 49-57.
11. Maas, L.C. and P.F. Renshaw, *Post-registration spatial filtering to reduce noise in functional MRI data sets.* Magn Reson Imaging, 1999. **17**(9): p. 1371-82.
12. Pluim, J.P., J.B. Maintz, and M.A. Viergever, *Interpolation artefacts in mutual information-based image registration.* Computer Vision and Image Understanding, 2000. **77**: p. 211-232.
13. Nickerson, L.D., et al., *Estimation of the local statistical noise in positron emission tomography revisited: practical implementation.* Neuroimage, 2003. **19**(2 Pt 1): p. 442-56.
14. Andersson, J.L. and S. Skare, *A Model-Based Method for Retrospective Correction of Geometric Distortions in Diffusion-Weighted EPI.* Neuroimage, 2002. **16**(1): p. 177-99.
15. Haselgrove, J.C. and J.R. Moore, *Correction for distortion of echo-planar images used to calculate the apparent diffusion coefficient.* Magn Reson Med, 1996. **36**(6): p. 960-4.
16. Horsfield, M.A., *Mapping eddy current induced fields for the correction of diffusion-weighted echo planar images.* Magn Reson Imaging, 1999. **17**(9): p. 1335-45.
17. Mangin, J.F., et al., *Distortion correction and robust tensor estimation for MR diffusion imaging.* Med Image Anal, 2002. **6**(3): p. 191-8.
18. Bastin, M.E., *Correction of eddy current-induced artefacts in diffusion tensor imaging using iterative cross-correlation.* Magn Reson Imaging, 1999. **17**(7): p. 1011-24.
19. Rohde, G.K., et al., *Comprehensive approach for correction of motion and distortion in diffusion-weighted MRI.* Magn Reson Med, 2004. **51**(1): p. 103-14.
20. Basser, P.J., J. Mattiello, and D. LeBihan, *Estimation of the effective self-diffusion tensor from the NMR spin echo.* J Magn Reson B, 1994. **103**(3): p. 247-54.
21. Studholme, C., R.T. Constable, and J.S. Duncan, *Accurate alignment of functional EPI data to anatomical MRI using a physics-based distortion model.* IEEE Trans Med Imaging, 2000. **19**(11): p. 1115-27.
22. Meijering, E.H., W.J. Niessen, and M.A. Viergever, *Quantitative evaluation of convolution-based methods for medical image interpolation.* Med Image Anal, 2001. **5**(2): p. 111-26.
23. Hogg, R.V. and A.T. Craig, *Expectations of Functions of Random Variables*, in *Introduction to Mathematical Statistics*, R.W. Pirtle, Editor. 1995, Prentice-Hall, Inc: Upper Saddle River, NJ.
24. Pierpaoli, C., et al., *Diffusion tensor MR imaging of the human brain.* Radiology, 1996. **201**(3): p. 637-48.
25. Haacke, E.M., et al., *Magnetic Resonance Imaging : Physical Principles and Sequence Design.* 1999, New York: Wiley-Liss.
26. Behrens, T.E., et al., *Characterization and propagation of uncertainty in diffusion-weighted MR imaging.* Magn Reson Med, 2003. **50**(5): p. 1077-88.
27. Shrager, R., et al. *When is a Gaussian displacement distribution adequate to describe water diffusion in tissues?* in *Workshop on Diffusion MRI: Biophysical Issues*. 2002. Saint-Malo, France: ISMRM.
28. Alexander, D.C., G.J. Barker, and S.R. Arridge, *Detection and modeling of non-Gaussian apparent diffusion coefficient profiles in human brain data.* Magn Reson Med, 2002. **48**(2): p. 331-40.
29. Chang, L.-C., et al. *RESTORE: Robust Estimation of Tensors by Outlier Rejection*. in *12th annual meeting of ISMRM*. 2004. Kyoto, Japan.
30. Maier, S.E., H. Mamata, and R.V. Mulkern, *Characterization of normal brain and brain tumor pathology by chisquares parameter maps of diffusion-weighted image data.* Eur J Radiol, 2003. **45**(3): p. 199-207.